

一般セッション(口頭講演) | 4 JSAP-Optica Joint Symposia 2024 : 4.1 Plasmonics and Nanophotonics

📅 2024年9月16日(月) 13:00 ~ 17:00 🏢 B4 (展示ホールB)

[16p-B4-1~13] 4.1 Plasmonics and Nanophotonics

Verma Prabhat(阪大)、田中 拓男(理研)

◆ 英語発表

13:00 ~ 13:30

[16p-B4-1]

[JSAP-Optica Joint Symposia Invited Talk] Plasmonic nanowire based intracellular material delivery

○Tomoko Inose^{1,2,3} (1.Kyoto Univ., 2.iCeMS, Kyoto Univ., 3.JST PRESTO)

◆ 英語発表

13:30 ~ 14:00

[16p-B4-2]

[JSAP-Optica Joint Symposia Invited Talk] Controlling lyotropic liquid crystalline self-assembly for creating nano carriers for biomedical applications

○Nhiem Tran¹ (1.RMIT University)

◆ 英語発表

14:00 ~ 14:15

[16p-B4-3]

Ultra-wide dynamic structural colors with width-modulated Cr-subwavelength grating on Ni/SiO₂ films○Yuusuke Takashima^{1,2}, Kentaro Nagamatsu^{1,2}, Yoshiki Naoi^{1,2} (1.Tokushima Univ., 2.pLED, Tokushima Univ.)

◆ 英語発表

14:15 ~ 14:30

[16p-B4-4]

Spectroscopic thermal emitters based on bimetallic compounds for high temperature plasmonic applications

○Andrea RuizPerona^{1,2}, Toan Tran Phuoc¹, Thien Duc Ngo¹, Tadaaki Nagao^{1,2} (1.NIMS, 2.Hokkaido Univ.)

◆ 英語発表

14:30 ~ 14:45

[16p-B4-5]

Designing Reconfigurable Metamaterials Toward Structural Color Generation

M. Pourmand¹, ○Pankaj Kumar Choudhury² (1.Umea University, 2.Zhejiang University)

◆ 英語発表

14:45 ~ 15:00

[16p-B4-6]

Investigation of Plasmonic Effect in Slot Rectangular Waveguide by Applying a Gold as Metal Optimization

○(D)Km Priyanka¹, Ritu Raj Singh¹ (1.NETAJI SUBHAS UNIVERSITY OF TECHNOLOGY, NEW DELHI)

◆ 奨励賞エントリー ◆ 英語発表

15:15 ~ 15:30

[16p-B4-7]

【No-Show】 Capillary-Interactions based Single-step and Scalable Fabrication of Gap-tuneable Plasmonic Nanostructures

○(DC)Renu Raman Sahu¹, Alwar Samy Ramasamy¹, Tapajyoti Das Gupta¹ (1.LANSPE, IAP, IISc)

◆ 奨励賞エントリー ◆ 英語発表

15:30 ~ 15:45

[16p-B4-8]

Self-Assembled Silicon Metasurface for Mechanically Tunable Optical Properties

○(M1)Yongan Hu¹, Patrick Probst¹, Mojtaba Karimi Habil¹, Hiroshi Sugimoto¹, Minoru Fujii¹ (1.Kobe Univ.)

◆ 奨励賞エントリー ◆ 英語発表

15:45 ~ 16:00

[16p-B4-9]

A Fano resonance enhanced surface plasmon sensing for IgG/anti-IgG immunosensor with high sensitivity

○(D)Yiming Lu^{1,3}, Hidekazu Ishitobi^{1,2,3}, Zouheir Sekkat^{4,5}, Yasushi Inouye^{1,2,3} (1.FBS, Osaka Univ., 2.Dept. of Appl. Phys. Osaka Univ., 3.PhotoBIO-OIL, AIST-Osaka Univ., 4.MAScIR, 5.Univ. Mohammed VI Polytechnic)

◆ 奨励賞エントリー ◆ 英語発表

16:00 ~ 16:15

[16p-B4-10]

Tunable abrupt autofocusing meta-devices

○(DC)Rong Lin¹, Mu Ku Chen¹, Din Ping Tsai¹ (1.CityU)

◆ 英語発表

16:15 ~ 16:30

[16p-B4-11]

Wavelength-multiplexed full color 3D metasurface hologram made of silicon nitride

○Tetsuhito Omori¹, Junpei Beppu¹, Masakazu Yamaguchi¹, Tamaki Onozawa¹, Kentaro Iwami¹ (1.TUAT)

◆ 英語発表

16:30 ~ 16:45

[16p-B4-12]

A Cost-Effective, Flexible 1D Metasurface Absorber in The Infrared Region

○(DC)Jhuma Pan¹, Sachin Kumar Srivastava¹ (1.IIT Roorkee)

◆ 英語発表

16:45 ~ 17:00

[16p-B4-13]

Polyaniline coated U-bent Fiber Optic Aptasensor for Arsenite Detection in Environmental Matrices

○(DC)Ashish Shukla¹, Tathagata Pal¹, Soumyo Mukherji¹ (1.IIT Bombay, Mumbai)

プラズモニックナノワイヤーを用いた細胞内物質導入技術の開発**Plasmonic nanowire based intracellular material delivery**京大白眉センター¹, 京大 iCeMS², JST さきがけ³ ○猪瀬 朋子^{1,2,3}Kyoto Univ.¹, JST PRESTO², °Tomoko Inose^{1,2}

E-mail: inose.tomoko.1v@kyoto-u.ac.jp

The technology for introducing biomolecules such as proteins and DNA into cells is widely used as a method to artificially control cell functions, ranging from basic biology to the pharmaceutical field. Methods employing liposomes, viral vectors, and the electroporation have been currently widely used, although these methods show low introduction efficiency or cell toxicity to some cell types. Another method for introducing biomolecules into cells is microinjection.¹⁾ This method physically introduces micro/nano needles directly into the cells, ensuring that biomolecules are reliably delivered within a cell.

Although several micro/nano needle methods have been reported, traditional micro/nano needles have limitations in the substances they can carry, posing challenges to their versatility. In this study, we developed a new method for introducing biomolecules into cells by applying the plasmonic nanowire single-cell endoscopy technique.²⁾ By utilizing the plasmonic effects occurring on nanowires, we have recently succeeded in controlling the spatiotemporal introduction of biomolecules into a single live cell.

- 1) Advanced tools and methods for single-cell surgery. A. Shakoor, W. Gao, L. Zhao, Z. Jiang, D. Sun , *Microsystems & Nanoengineering*, **2022**, 8, 47.
- 2) Live-Cell SERS Endoscopy Using Plasmonic Nanowire Waveguides. G. Lu, H. De Keersmaecker, L. Su, B. Kenens, S. Rocha, E. Fron, C. Chen, P. Van Dorpe, H. Mizuno, J. Hofkens, J. A. Hutchison, H. Uji-i, *Adv. Mater.*, **2014**, 26, 5124

Controlling lyotropic liquid crystalline self-assembly for creating nano carriers for biomedical applications

Nhiem Tran

School of Science, RMIT University, Melbourne, Victoria, Australia

nhiem.tran@rmit.edu.au

Abstract

Lipid nanoparticles (LNP) have been widely used as carriers for drugs and genes, including in mRNA-vaccines for COVID-19. A special class of LNP, lyotropic liquid crystalline LNP, comprise mainly of amphiphilic lipids self-assembling into two- and three-dimensional, inverse hexagonal, and cubic nanostructures (Fig. 1). Mesophase structures of self-assembled lyotropic liquid crystalline nanoparticles are important factors that directly influence their ability to encapsulate and release drugs and their biological activities.^{1,2} For example, the release rate of hydrophilic compounds was found to be much faster in the cubic phase than in the hexagonal phase, micellar cubic phase, and microemulsion.³ Additionally, it has been shown that the internal nanostructures also affect cellular response such as cell uptake of nanoparticles, hemolysis, and cytotoxicity.⁴ Importantly, the *in vivo* behavior of nanoparticles such as biodistribution appears to be regulated by their nanostructures.⁵ However, it is difficult to predict and precisely control the mesophase behavior of these self-assembled nanomaterials, especially in complex systems with several components.

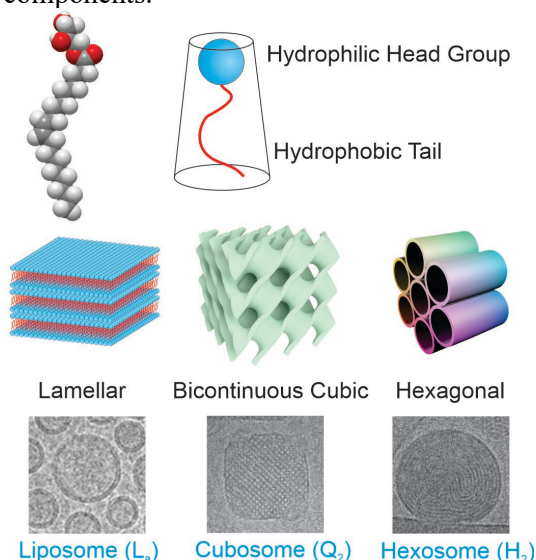


Figure 1. Molecular structure of monoolein, an amphiphile that can self-assemble into various mesophase structures, which can be dispersed and form nanoparticles including liposomes, cubosomes, and hexosomes.

In this presentation, a structural study of self-assembled lipid mesophase using synchrotron small angle X-ray scattering will be reported. Using the understanding of the lipid self-assembled structures, lipid nanoparticles with different internal nanostructures will be created to study their *in vitro* interaction with cells and *in vivo* biodistribution. Furthermore, formulation of “smart” LNP, which switch between structures in response to pH will be reported (Fig. 2). Since low pH conditions are observed in tumours and infected sites, an elevated release rate allows for better targeted therapies. Herein, pH responsive LNP containing novel ionisable lipids and their applications as carriers for anticancer and antimicrobial agents are reported.

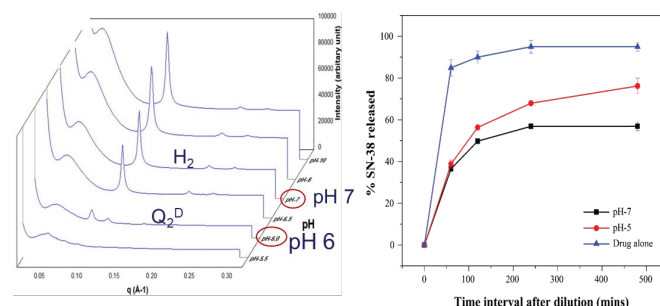


Figure 2: pH responsive LNP showing a hexagonal structure at pH 7 and a cubic structure at pH 6. When used to encapsulate anti-cancer drug SN-38, the structural difference at pH 5 and pH 7 resulted in varied drug release kinetics.⁶

References

1. Clogston, J. & Caffrey, M. J. Controlled Release 107, 97-111 (2005).
2. Zhai, J. et al. ACS nano 13, 6178-6206 (2019).
3. Phan, S. et al., I. J. Pharm. 421, 176-182 (2011).
4. Tan, A., et al. Adv. Sci. (2018).
5. Tran, N. et al. Mater. Sci. Eng.: C 71, 584-593 (2016).
6. Rajesh, S. et al. Pharmaceutics 2022, 14(10), 2175

Ultra-wide dynamic structural colors with width-modulated Cr-subwavelength grating on Ni/SiO₂ films

Yuusuke Takashima^{1,2}, Kentaro Nagamatsu^{1,2}, Yoshiki Naoi^{1,2}

¹ Faculty of Science and Technology, Tokushima University, Tokushima, Japan,

² Institute of Post-LED Photonics, Tokushima University, Tokushima, Japan

E-mail: takashima@tokushima-u.ac.jp.

1. Introduction

The structural color resulting from the interaction between light and artificially designed nanostructures is attractive for many fields including display, imaging, and security [1]. Dynamic control of the interaction significantly promotes the flexibility of design and is very important for the applications mentioned above. Many researchers tried to produce the dynamic structural color using mechanical displacement [2], polarization [3], and phase-change materials [4]. However, the color gamut from one design unit still be restricted. In this work, we demonstrated ultra-wide dynamic structural colors utilizing highly lossy metal/insulator/metal (MIM) structures with width-modulated subwavelength grating (SWG).

2. Results and discussions

Figure 1 shows a sketch of our proposed structure. A 100 nm-Ni and 65 nm-SiO₂ films were electron-beam (EB) evaporated onto the glass substrate. The 30 nm-thickness Cr-subwavelength grating (SWG) is formed by the EB lithography technique. The grating period is 400 nm. The designed structure supports spectrally broadened gap-plasmon resonance due to the strong damping of Cr and Ni. The spectrally broadened resonance also gives a large phase-retardation between orthogonal polarizations. When the polarized incident light with 45° to the grating bars is irradiated, the polarization of the reflected light is changed by the phase-retardation. Moreover, we employed two-type grating widths (210 nm/100 nm) to expand of the resonant bandwidth and induce the phase-retardation in further wide spectral region. Thus, ultra-wide tunability of the reflection color is expected by simply rotating the analyzing polarizer.

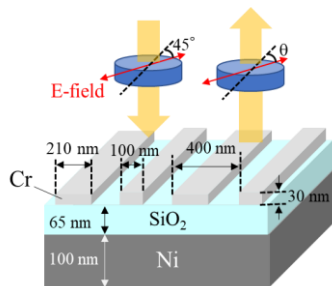


Figure 1 Schematic sketch of Ni/SiO₂/width-modulated Cr-SWG structure.

The normal reflection spectra from the fabricated sam-

ple at a certain analyzer angle θ are shown in Fig. 2 (a). For $\theta = 0^\circ$ (E-field is parallel to the grating bars, namely s-polarization), the reflection dip associated with destructive interference Air/SiO₂ and Ni/SiO₂ is obtained at 550 nm. In contrast, the reflectivity at $\theta = 90^\circ$ (namely, p-polarization) is decreased at the broad wavelength region around 600 to 700 nm because of excitation of gap plasmon mode. The excited gap plasmon mode also provides significant phase-retardation, and this modifies the polarization state of reflected light. Hence, the different colors from p- and s-polarization appear at $\theta = 45^\circ$ and 135° . Figure 2 (b) shows the gamut of the fabricated sample in CIE1931 color space (the conversion used standard illuminant D65 and 2° observer color-matching function). When rotating the analyzer, the gamut shows an ultra-wide oval covering the whole visible region. The tunable range covers 37% of the sRGB area by only one design unit, and we demonstrated a wider dynamic range than previous reports [3,4].

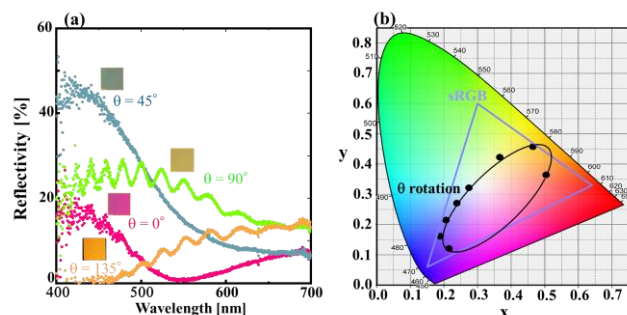


Figure 2 (a) Normal reflection spectra from the fabricated Ni/SiO₂/width-modulated Cr-SWG at various analyzing polarizer angle θ (b) Color gamut of our structure in CIE1931 color space.

3. Conclusions

Ultra-wide polarization-tunable structural color was demonstrated using spectrally broadened resonance in Ni/SiO₂/width-modulated Cr-SWG. This wide-tunability is very attractive for the design of many applications.

Acknowledgements

This work is supported in part by JSPS KAKENHI JP24K1731100.

References

- [1] D. Wang *et al.*, *Nanophotonics* **12** (2023) 1019.
- [2] A. L. Holsteen *et al.*, *Science* **365** (2019) 257.
- [3] X. Shang *et al.*, *Photonics* **10** (2023) 448.
- [4] F. Shu *et al.*, *Adv. Opt. Mater.* **6** (2018) 1700939.

Spectroscopic thermal emitters based on bimetallic compounds for high temperature plasmonic applications

NIMS¹, Hokkaido Univ.², [○]Andrea Ruiz-Perona^{1,2}, Toan Tran Phouc^{1,2}, Thien Duc Ngo¹, Tadaaki Nagao^{1,2*}

Email: NAGAO.Tadaaki@nims.go.jp

Metallic refractory materials, such as single-element metals, bimetallic alloys, metal borides, and metal silicides, are attracting increasing interest and usage in industrial furnaces, aerospace technology, and energy harvesting, due to their outstanding chemical and structural stability at high temperatures. Nevertheless, their optical properties are much inferior in comparison to representative plasmonic metals like Au, Cu, or Al, which, in contrast, exhibit lower melting points and are susceptible to oxidation, thereby hindering the development of thermophotonics applications in high-temperature environments.

Spectroscopic infrared thermal emitters selectively emit or absorb infrared radiation with very narrow spectral resolution, making them increasingly appealing for applications such as plasmon-enhanced vibrational spectroscopy, material-selective heating/drying systems, thermophotovoltaics, or spectroscopic infrared light sources in gas sensors. Consequently, there is an increasing need to find materials with a strong plasmonic response and high-temperature stability suitable for use in high-temperature photo-energy applications, such as thermal emitters or thermal detectors. We propose binary metallic compounds such as nickel-based superalloys as promising candidates for photothermal applications due to their high oxidation resistance in air and good optical performance.

In this study, nickel aluminum (NiAl) thin films are fabricated via direct current (DC) sputtering deposition under different growth conditions. These layers grow in unique uniaxial fashion, which yields high crystallinity and results in strong plasmonic polarizability within the IR spectral region. Simulations of plasmonic thermal emitters based on our material's optical properties have reached absorptivity/emissivity values close to 1 for targeted wavelengths. Plasmonic emitter devices following the simulation parameters are fabricated to demonstrate the optical performance of the materials. The experimental results demonstrate the applicability of nickel-based alloys similar to the case of metal borides for high-temperature plasmonic applications in vacuum as well as in atmosphere.

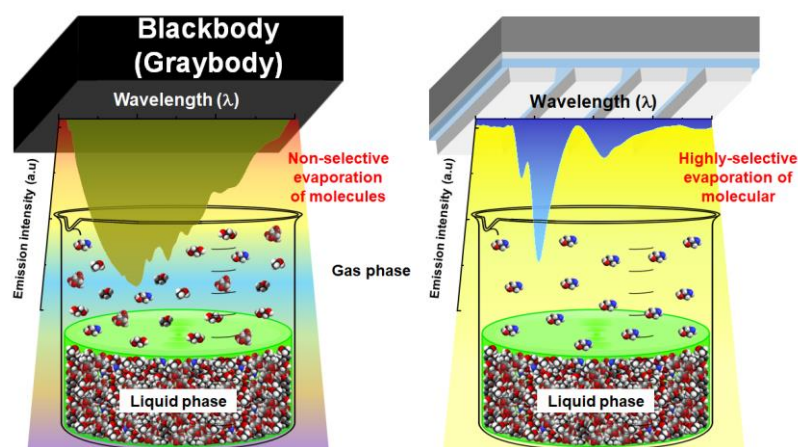


Fig. 1. Example of use of wavelength-selective thermal emitters.

[1] T.P. Tran, T.D. Ngo, H.D. Ngo, T. Nagao, Appl. Phys. Express **14**, 087001 (2021).

[2] P.T. Tran, D.T. Ngo, H.D. Ngo, O.S. Handegård and T. Nagao, Optics Express **30**, 38630 (2022).

Designing Reconfigurable Metamaterials Toward Structural Color Generation

M. Pourmand¹ and Pankaj K. Choudhury^{2*}

¹Department of Applied Physics and Electronics, Umeå University, SE-901 87 Umeå, Sweden

²International Research Center for Advanced Photonics, Zhejiang University, Haining 314400, China

*E-mail: pkchoudhury@icape.org

1. Introduction

Dynamic color-generation structures provide higher resolution and scalability compared to the traditional pigmentation-based displays [1]. The main roadblock to the wide adoption of structural colors is the fixed optical response after the realization process. To address this issue, several kinds of tunability mechanisms have been introduced including the implementation of plasmonic nano-antennas enabled by liquid crystals [2] and plasmonic resonators exploiting stretchable materials [3]. The chalcogenide phase-change mediums- (PCMs) based plasmonic structures [4–6] offer advantages including flexibility, color durability, high resolution, cost-effectiveness, and CMOS compatibility [7]. Herein, we propose an optimized PCM-integrated structure to generate a wide spectrum of colors.

2. Structural Configuration

Figure 1 illustrates the structure comprising n bilayers of GeSe₃ (of thickness d_D^n) and Al (of thickness d_m^n). To thermally excite the structure, we use a 1 nm thick heating layer of tri-layer graphene. The SiO₂ layers on the top and bottom of the structure have their own merits. The capping SiO₂ layer protects the GeSe₃ medium from evaporation, and the SiO₂ buffer layer above the substrate isolates graphene sheets from the metallic layer above. Also, it provides sufficient adhesion between the graphene sheet and SiO₂ substrate during the fabrication process. Furthermore, the structure can be fabricated by using lithography-free techniques, such as the physical vapor deposition (PVD) method, namely thermal evaporation and/or RF sputtering [8].

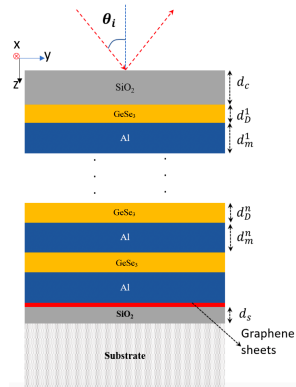


Fig. 1. Two-dimensional schematic of the proposed structure.

3. Results and Discussion

Figure 2 illustrates the reflection spectra of the optimized configuration, wherein we demonstrate the generation of primary colors (red, green, and blue) by the optimized structures corresponding to the amorphous and crystalline states of GeSe₃. It is obvious that the peak reflectance has values

above 0.6 in all structural configurations. Moreover, the reflectivity undergoes a blue shift upon transition of the phase of GeSe₃ from amorphous to crystalline.

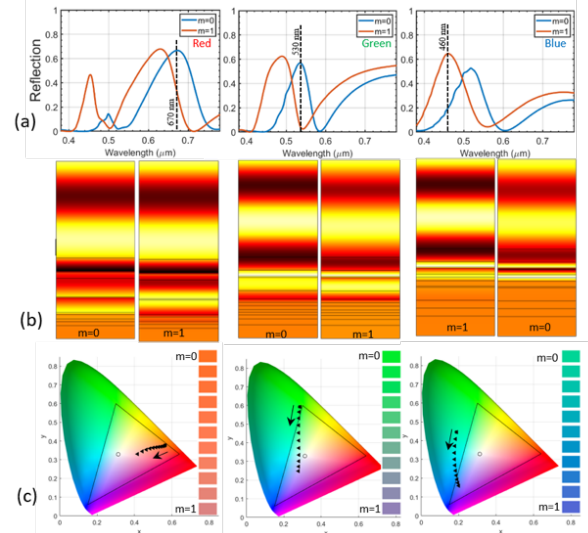


Fig. 2. Spectral features of the optimized structure for the fully amorphous ($m = 0$) and fully crystalline ($m = 1$) states of GeSe₃ medium in the configuration. (a) Reflection spectra for the red (left), green (center), and blue (right) pixels for the amorphous and crystalline states of GeSe₃; dashed lines denote the target wavelengths of primary colors considered in the optimization process. (b) Distribution of magnetic field at the target wavelengths of primary colors. (c) The trajectory of reflected colors as a function of m .

4. Conclusion

A reconfigurable layered metamaterial configuration comprising GeSe₃/Al bilayer stacks has been investigated. The implemented design optimization exhibits the generation of primary colors, i.e., the red, green, and blue pixels. The embedded graphene micro-heater facilitates control over the ambient temperature upon being excited due to external electrical pulses, which ultimately governs the pixel-sized tunability of the reflected color. The proposed layered configuration has potential in designing reflective display systems.

Acknowledgement

PKC acknowledges the financial support by Zhejiang University (China) through the grant 11133000*194232301/002.

References

- [1] A. Kristensen et al., *Nature Rev. Mater.* **2** (2016) 16088.
- [2] D. Franklin et al., *Nature Commun.* **6** (2015) 7337.
- [3] B. H. Miller, H. Liu, and M. Kolle, *Nature Mater.* **21** (2022) 1014.
- [4] M. Pourmand and P. K. Choudhury, *J. Opt. Soc. Am. B* **39** (2022) 1222.
- [5] M. Pourmand and P. K. Choudhury, *IEEE Trans. Nanotechnol.* **21** (2022) 586.
- [6] M. Pourmand and P. K. Choudhury, *J. Opt. Soc. Am. B* **40** (2023), 1625.
- [7] M. Wuttig et al., *Nature Photon.* **11** (2017) 465.
- [8] S. S. Ghazi et al., *Nano Lett.* **19**, (2019) 7377.

Investigation of Plasmonic Effect in Slot Rectangular Waveguide by Applying a Gold as Metal Optimization

Km Priyanka^{1,*}, Ritu Raj Singh¹

¹Department of Electronics and Communication Engineering, Netaji Subhas University of Technology, Delhi, India.

E-mail: km.priyanka.phd22@nsut.ac.in

Introduction

Surface plasmon polaritons (SPPs) are the electromagnetic excitations that evaporate when confined in a direction perpendicular to the interface and propagate along the interface between two different media with opposite dielectric constants in a wave-like pattern [1]. It gives a strong light confinement power in integrated photonic circuit [2]. In this paper, by using SoI technology light confinement for the plasmonic slot rectangular waveguide is studied. The most promising dimension of the recommended design is represented by the values of d_3 and d_4 , which are 180 nm and 220 nm, respectively, for the waveguide's width and height [3]. The slot rectangular waveguide confinement power and mode effective area are studied by applying a Gold (Au) layer around the core at a distance M_g .

Structure

The cross-sectional and three-dimensional (3-D) views of the slot rectangular silicon on insulator waveguide (SRSOIW) structural design are displayed in Fig. 1(a) and (b). The thickness of metal (Δt) is taken 100 nm [4]. With coherent oscillations of free electrons between metal dielectric surface, surface plasmon waves are conceptualized. The waveguide design consists of SiO_2 as substrate, Au as a plasmon and Si as core material. At operating wavelength taken as 1550 nm, the Refractive index (RI) of substrate and core are 1.44 and 3.47 respectively. Additionally, the Johnson and Christy model [5] is used to incorporate the RI of the Au layer.

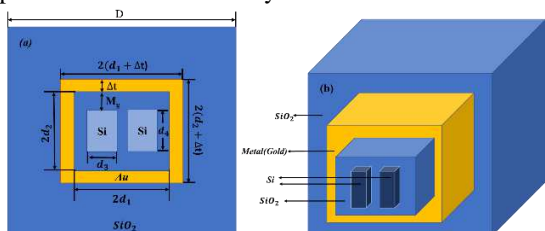


Fig. 1 (a) Cross sectional view and (b) 3-D view of plasmonic based slot rectangular waveguide.

Result and discussion

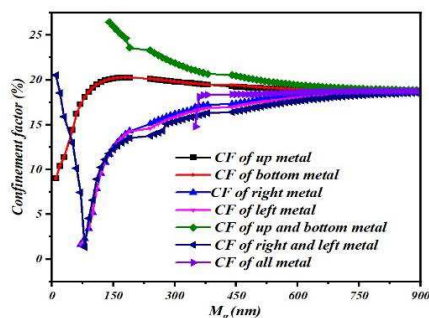


Fig. 2 Confinement factor for optimization of the M_g .

After investigating the plasmonic effect of Si material, Fig. 2 represents the variation of the metal gap (M_g) with respect to the confinement factor (CF). It reveals that CF saturates at 900 nm, and at this point, there is strong light-confinement in the slot region which is required for the propagation of the light in the slot.

Considering CF, $M_g = 900$ nm, comes out to be optimum value for placing the metal.

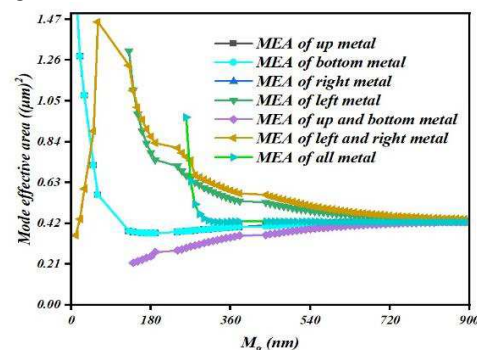


Fig. 3 Mode effective area for optimization of the M_g .

Similarly, in Fig. 3, the Mode Effective Area (MEA) is $0.44 \mu\text{m}^2$ for all Au layers at $M_g = 900$ nm. Considering MEA, the optimal value for M_g comes out to be ~ 900 nm. The optimization of the structure is to maximize the CF and minimize MEA.

Conclusion

Using the Finite Element Method (FEM), the plasmonic slot rectangular waveguide with Gold (Au) placed at all sides of the core at distance (M_g) is examined. The CF and MEA obtained as $\sim 18.75\%$ and $\sim 0.44 \mu\text{m}^2$ at the distance (M_g) of 900 nm. Hence, the optimal value to place a metal layer from the core is approx. 900 nm is achieved for this waveguide. The goal of using metal in a waveguide for strong light confinement with low loss is best achieved at this distance.

Reference

- [1] S. Kumari, R. R. Singh, and S. M. Tripathi, "Parametric Optimization of Hybrid Plasmonic Waveguide-Based SOI Ring Resonator Refractive Index Sensor," *Plasmonics*, vol. 17, no. 6, pp. 2417–2430, Dec. 2022, doi: 10.1007/s11468-022-01724-6.
- [2] B. Banan, M. S. Hai, E. Lisicka-Skrzek, P. Berini, and O. Liboiron-Ladouceur, "Multichannel Transmission Through a Gold Strip Plasmonic Waveguide Embedded in Cytosol," *IEEE Photonics J.*, vol. 5, no. 3, pp. 2201811–2201811, Jun. 2013, doi: 10.1109/JPHOT.2013.2267537.
- [3] S. Vardhan and R. R. Singh, "Optimization and Comparative Analysis of Rectangular and Slot Waveguide based Symmetric Ring and Racetrack Resonators for SoI Photonic Integrated Filters," *Silicon*, vol. 16, no. 7, pp. 2913–2926, May 2024, doi: 10.1007/s12633-024-02879-z.
- [4] S. H. Badri and M. M. Gilarlue, "Coupling Between Silicon Waveguide and Metal-Dielectric-Metal Plasmonic Waveguide with Lens-Funnel Structure," *Plasmonics*, vol. 15, no. 3, pp. 821–827, Jun. 2020, doi: 10.1007/s11468-019-01085-7.
- [5] P. Joensen, J. C. Irwin, J. F. Cochran, and A. E. Curzon, "Transmission method for determining the optical constants of metals," *J. Opt. Soc. Am.*, vol. 63, no. 12, p. 1556, Dec. 1973, doi: 10.1364/JOSA.63.001556.



Capillary-Interactions based Single-step and Scalable Fabrication of Gap-tuneable Plasmonic Nanostructures

(DC) Renu Raman Sahu¹, Alwar Samy Ramasamy², Tapajyoti Das Gupta³

Lab. of Adv Nanostructures for Photonics and Electronics^{1, 2, 3}, Instrumentation and Applied Physics,

Indian Institute of Science, C. V. Raman Road, Bengaluru, India, 560012

E-mail: renuraman@iisc.ac.in

Abstract: A scalable and single-step method (Fig 1a) exploiting capillary interactions (Fig 1b) for creating sub-100nm (Fig 1c, 1d) non-coalescent metallic(Ga) nanodroplets on Polydimethylsiloxane (PDMS), a bio-compatible elastomeric substrate, is shown herein. The nanoscale gap between Gallium nanodroplets thus formed allows for spectrally dependent electric field enhancement (Fig 1e), owing to plasmon hybridization of neighboring Ga nanodroplets. The substrate, PDMS, allows not only for gap tuneability but also actively participates in determining the Ga nanosphere sizes. It thus enables numerous potential technologies involving mechanochromic sensing (Fig 1f, 1g) and display applications (Fig 1h).

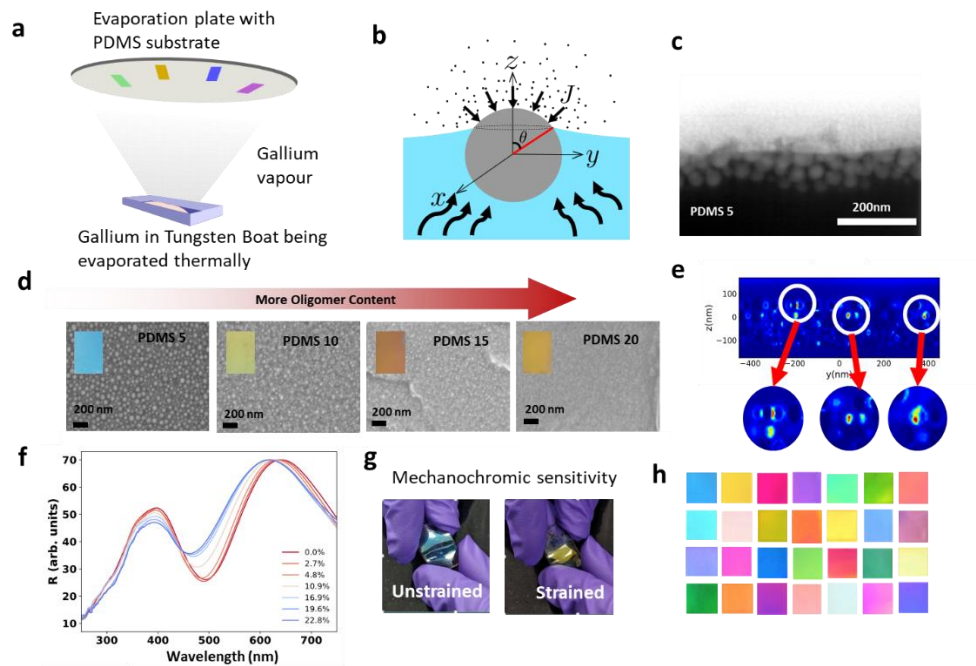


Figure 1: a. Thermal evaporation of Ga onto PDMS with different oligomer content. b. Capillary interaction of Ga and liquid oligomers results in the growth of nanodroplets and encapsulation by the liquid oligomers. c. The cross-section image of Ga nanodroplets on PDMS. d. Top-view image of Ga nanodroplets on PDMS, showing different size distributions as the oligomer content varies. (inset) Optical images of real samples. e. Gap plasmon resonances excited in the inter-droplet gaps. f. The reflectivity spectra of Ga-on-PDMS sample for different strain values. The blue shift in the visible region is a result of gap plasmon resonances, whereas UV spectral features are due to scattering by individual Ga nanodroplets, unchanging with strain. g. Sample changing its color from blue to yellow on mechanical deformation. h. Palette of samples with Ga-on-PDMS based structural colors, fabricated by the capillary interactions of liquid Ga and liquid-oligomers of PDMS.

Self-Assembled Silicon Metasurface for Mechanically Tunable Optical Properties

Yongan Hu, Patrick T. Probst, Mojtaba Karimi Habil, Hiroshi Sugimoto, Minoru Fujii

Kobe University,
E-mail: sugimoto@eedept.kobe-u.ac.jp

1. Introduction

The metasurface approach is an effective way to manipulate light at the nanoscale. Dielectric metasurfaces benefit from low losses as compared to their plasmonic counterpart, which comprises metal nanoparticles. Moreover, Mie-resonant dielectric metasurfaces support magnetic resonances in addition to electric ones. In a 2D array, the resonance from the individual nanoparticles interferes with the Rayleigh anomalies (RAs) of the periodic structure to produce a collective surface lattice resonance (SLR). In-situ control over this lattice resonance can be realized by employing external stimuli like mechanical deformation.^[1] Due to its elastic, inert and nontoxic properties, PDMS is popular as stretchable substrate. Conventionally, 2D metasurface arrays are fabricated via electron beam lithography. Nevertheless, this method is time-consuming, requires expensive facilities and is challenging to combine with stretchable substrates.

In this work, we present a mechanically tunable 2D Si nanoparticle array produced via templated colloidal self-assembly on a PDMS substrate. We successfully excite the collective electric dipole resonance in the periodic array. Stretching the elastic substrate shifts the spectral position of the resonance by tuning the periodicity. When the collective resonance overlaps with the single-particle magnetic resonance, the lattice Kerker effect arises and the reflectivity is strongly reduced.

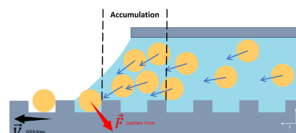
2. Results

The tunable 2D array is fabricated by assembling colloidal Si nanoparticles inside a PDMS nanohole array, via template-assisted self-assembly,^[2,3] as shown in Figure 1a. Stretching the elastic substrate is accomplished with a customized device to tune the periodicity of the 2D array. Figure 1b shows a dark field image of the highly filled 2D array. The average diameter of Si nanoparticles and the periodicity of the unstrained sample are 116 nm and 550 nm, respectively.

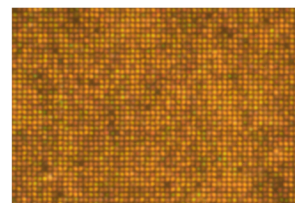
The optical properties of 2D array with smaller periodicity of 300 nm under different strains are studied using an optical microscope. Figure 1c and Figure 1d show the measured and simulated reflection spectra of the 2D Si nanoparticle array under various strains. Here, the specified strain indicates the change in periodicity relative to the original particle-to-particle distance of 300 nm. The spectra show good agreement with the simulations: the collective electric dipole lattice resonance (ED-LR) shifts from around 460 nm to 500 nm. At 50 nm strain, it overlaps with the magnetic dipole (MD) resonance, which results in the suppression of the reflection by the lattice Kerker effect. For

the strain beyond 50 nm, the collective electric dipole resonance further red-shifts and becomes broader with lower intensity.

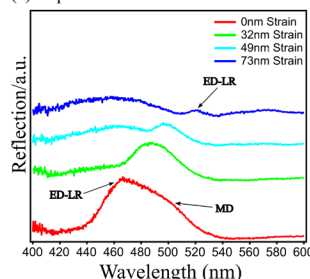
(a) Self-assembly



(b) Dark field image of the Si nanoparticles 2D array



(c) Experiment



(d) Simulation

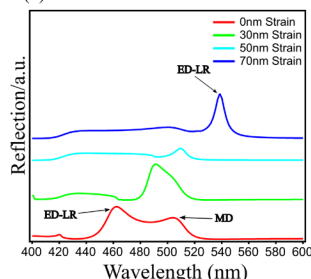


Figure 1. (a) Schematic illustration of template-assisted self-assembly. (b) Dark field image of the Si nanoparticle 2D array. (c) Experimental and (d) simulated reflection spectra of the Si nanoparticles 2D array under different strains, the arrows indicate the spots of the collective electric dipole resonance (ED-LR) and the magnetic dipole resonance (MD).

3. Conclusion

We have successfully fabricated a high-quality 2D array of Si nanoparticles on a PDMS substrate via colloidal self-assembly. By applying tensile strain to the substrate, we have succeeded in tuning the lattice constant and to adjust the electric dipole lattice resonance to match the magnetic one, which suppressed the reflection by the lattice Kerker effect.

References

- [1] Yonghao Cui, et al., ACS Nano 2012 6 (3), 2385-2393
- [2] Gupta, V., Probst, P. T., et al., ACS Appl. Mater. 2019, 11, 28189–28196.
- [3] H. Negoro, et al., Adv. Opt. Mater. 10 (2022), 2102750.

A Fano resonance enhanced surface plasmon sensing for IgG/anti-IgG immunosensor with high sensitivity

○(D)Lu Yiming^{1,3}, Hidekazu Ishitobi^{1,2,3}, Zouheir Sekkat^{4,5}, Yasushi Inouye^{1,2,3}

FBS, Osaka Univ.¹, Dept. of Appl. Phys. Osaka Univ.², PhotoBIO-OIL, AIST-Osaka Univ.³, MAScIR⁴,
University Mohammed VI Polytechnic⁵
E-mail: Lu_Yiming@ap.eng.osaka-u.ac.jp

1. Introduction

Surface plasmon resonance (SPR) is widely used as a label-free method for monitoring molecular interactions such as antigen-antibody interactions by measuring the shift in the SPR angle due to changes in the refractive index of the sensing surface. Recently, SPR sensors based on Fano resonance have been proposed to improve the sensitivity of SPR sensors [1]. In our previous report, SF11/Ag/SiO₂/TiO₂ multilayer system for Fano resonant SPR was developed and applied to the detection of glucose concentration, successfully improving the sensitivity by about one order of magnitude [2].

In this study, the SF11/Ag/SiO₂/TiO₂ Fano multilayer system was investigated to be extended to the monitoring of molecular interactions such as antigen-antibody interactions. In particular, the interaction between immunoglobulin G (IgG) and anti-IgG was to be examined.

2. Methods and Results

At first, SF11/Ag/SiO₂/TiO₂ multilayer Fano substrates were prepared by sequential deposition by sputtering method. Then, a surface modification process was investigated to immobilize IgG on the SF11/Ag/SiO₂/TiO₂ Fano substrates (Fig. 1). ATR spectra of the modified Fano substrates were subsequently measured under conditions of pure water, IgG solution and anti-IgG solution, respectively, as shown in Fig. 2. In pure water, an asymmetric Fano dip was observed around 60.59° angle of incidence, whereas in the 50 µg/mL IgG solution, the Fano dip was shifted towards the 0.12° higher angle. As the solution was changed from 50 µg/mL IgG solution to 55 µg/mL anti-IgG solution, a further shift of ca. 0.12° to the higher angle side was seen. The refractive index and thickness of the IgG and anti-IgG layers were also determined using numerical analysis based on Fresnel formulae.

3. Conclusion

We have prepared SF11/Ag/SiO₂/TiO₂ substrates for Fano resonance SPR measurements

and developed a surface modification method for monitoring intermolecular interactions. An experimental scheme for detecting IgG/anti-IgG interactions was thereby established. Evaluation of the detection limit of this method, improvement of sensitivity by reducing the extinction coefficient of the TiO₂ layer and improvement of the chemical stability of the substrate surface are to be investigated.

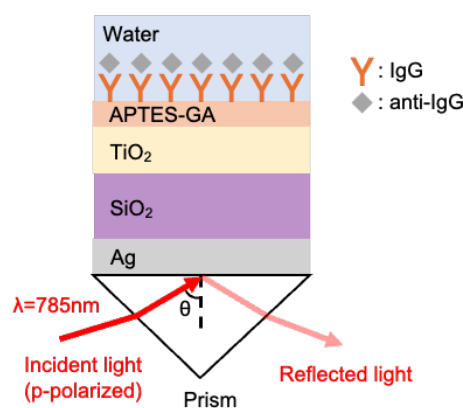


Figure1 Structure of modified SF11/Ag/SiO₂/TiO₂ multilayer Fano substrate

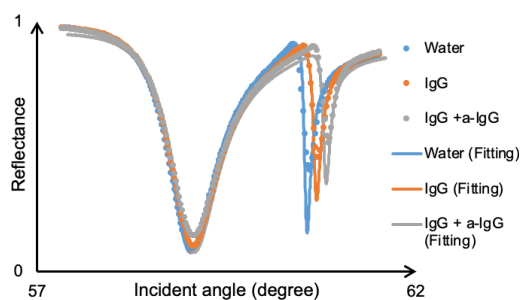


Figure2 ATR spectra and fitting curve of modified SF11/Ag/SiO₂/TiO₂ substrate under the condition of water, 50 µg/mL IgG solution and 55 µg/mL anti-IgG solution

References

- [1] S. Hayashi et al., Sci. Rep. **6** (2016) 33144.
- [2] T. Ishizu et al., 21a-A200-2, the 83rd JSAP Autumn Meeting (2022).

Tunable abrupt autofocusing meta-devices

Rong Lin¹, Mu Ku Chen^{1,2,3}, Din Ping Tsai^{1,2,3}

¹ Department of Electrical Engineering, City University of Hong Kong, Kowloon, Hong Kong SAR 999077, China

² Centre for Biosystems, Neuroscience, and Nanotechnology, City University of Hong Kong, Kowloon, Hong Kong SAR 999077, China

³ The State Key Laboratory of Terahertz and Millimeter Waves, City University of Hong Kong, Kowloon, Hong Kong SAR 999077, China

E-mail: rong.lin@my.cityu.edu.hk

1. Introduction

Abrupt autofocusing (AAF) beams [1], integrating features of circular Airy and Bessel beams, offer extended focal depths, self-healing properties, high precision, and minimal energy loss. These qualities make them ideal for advanced optical imaging, particle trapping, and laser surgery. Traditionally, spatial light modulators (SLMs) have been used to generate AAF beams by encoding their Fourier transform. However, SLMs suffer from low resolution, energy inefficiency, and a limited operational wavelength range, which hinder precise nanoscale operations. Additionally, their bulky size is at odds with the trend towards device miniaturization and integration. Metasurfaces [2-4], capable of manipulating wavefronts at subwavelength scales, present a superior alternative to traditional optical devices by offering reduced weight, increased efficiency, smaller size, and lower energy consumption. Metasurfaces have found applications [5-7] in beam shaping, achromatic imaging, light-field sensing, holography, optical computing, quantum technologies, and biological imaging. Yet, challenges remain in biomedical applications, particularly in creating dynamic beams essential for improving image contrast, optical tweezing, and optimizing photodynamic therapy.

In this research, we introduce two types of tunable abrupt autofocusing meta-devices composed of dual metasurfaces. By adjusting the relative rotation between these metasurfaces, one device can dynamically steer the AAF beam, while the other adjusts its focal length. Importantly, these tuning methods are wavelength-independent and scalable. We anticipate that these tunable meta-devices will significantly advance the use of AAF beams in precise biomedical applications such as laser therapy, particle manipulation, and biological imaging.

2. Results

The capability to generate tunable abrupt autofocusing beams relies on the precise superposition of phase profiles. Take AAF beam with steered angles as an example, the Fourier transform of an AAF beam should be added on the first metasurface. To realize the dynamic steering function, a gradient phase distribution can be introduced and decomposed into two distinct phase profiles of off-axis Fresnel lenses. Fig. 1 shows the schematic diagram of tunable abrupt autofocusing meta-devices.

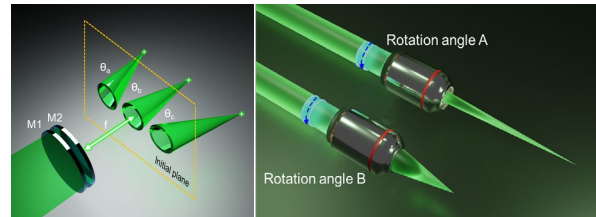


Fig. 1. Schematic diagrams of tunable abrupt autofocusing meta-devices. (Left) Steered AAF beam generation; (Right) Vari-focal AAF beam generation.

It should be emphasized that any discrepancies, such as gaps, mismatches, and fabrication defects, can significantly impair the performance of beam steering and autofocusing. Therefore, it is advisable to construct the metasurfaces with a larger scale and minimize the distance between them to reduce wavefront fluctuations as much as possible.

3. Conclusions

To summarize, we employed the superimposed phase method to design metasurfaces capable of generating an AAF beam and dynamically tuning the deflection angle or the focal length. We believe that this work clearly reveals one of the tunability methods within the field of metasurfaces and enhances the functionality of AAF beams, which benefits the possibility of application in bioimaging, biomedical applications, and laser surgery.

Acknowledgements

This work is supported by the University Grants Committee / Research Grants Council of the Hong Kong Special Administrative Region, China [Project No. AoE/P-502/20, CRF Project: C1015-21E; C5031-22G, GRF Project: CityU15303521; CityU11305223; and Germany/Hong Kong Joint Research Scheme: G-CityU 101/22], City University of Hong Kong [Project No. 9380131, 9610628, and 7005867], and National Natural Science Foundation of China [Grant No. 62375232].

References

- [1] Nikolaos K. Efremidis, *Optica* 6 (2019) 686.
- [2] Shuming Wang, *Nat. Nanotech.* 13 (2018) 227.
- [3] Jin Yao, *Adv. Photonics* 5 (2023) 024001.
- [4] Yuan Luo, *Small Methods* 6 (2022) 2101228.
- [5] Rong Lin, *J. Phys. D Appl. Phys.* 54 (2021) 145108
- [6] Rong Lin, *Opt. Express* 29 (2021) 30357
- [7] Rong Lin, *J. Phys. Chem. C* 128 (2024) 7661

Wavelength-multiplexed full color 3D metasurface hologram made of silicon nitride

Tetsuhito Omori, Junpei Beppu, Masakazu Yamaguchi, Tamaki Onozawa, and Kentaro Iwami

Tokyo University of Agriculture and Technology

E-mail: omori@st.go.tuat.ac.jp

1. Introduction

Metasurface holograms, which enable a wide viewing angle and high resolution by using subwavelength-sized nanostructures, are expected to be applied to 3D displays^[1]. In our previous studies, full-color 2D holograms^[2] and large-area monochromatic 3D holograms^[3] have been achieved. In this research, we have proposed a method to reproduce a full-color 3D image without misalignment by integrating the phase distribution of each RGB into a single hologram as a matrix of phase vectors $\phi_{All} = (\phi_B, \phi_G, \phi_R)$ as shown in Fig. 1.

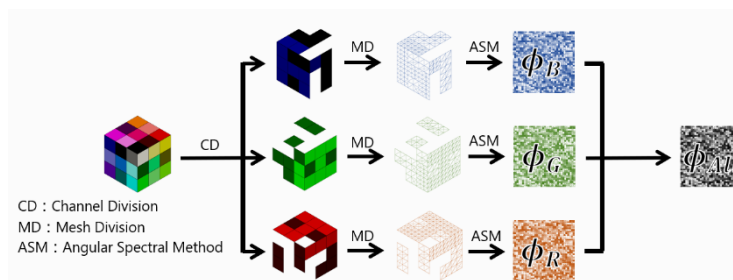


Fig. 1 Method for making holograms

2. Design and simulation

Silicon nitride (SiN) pillars with various cross-sectional shapes were adopted as meta-atoms. As shown in Fig. 1, first, the surfaces of an artificial 3D object was decomposed into each RGB color channels, and the intensity of each channel was converted to mesh density. Then, the phase distributions for each channel was calculated using the angular spectrum method. The propagation distance and the deflection angle were set to 10 mm and 20°, respectively, to prevent overlap with the conjugate image. Finally, meta-atoms that could reproduce the phase vector $\phi_{All} = (\phi_B, \phi_G, \phi_R)$ were selected from the library with approximately 20,000 species using the least square errors method.

We then simulated the reproduction of a target image shown in Fig. 2. Simulation based on our meta-atom library with the phase coverage of Fig. 3(a) shows the limited color reproduction with a peak signal-to-noise ratio (PSNR) of 27.9 dB, as shown in Fig. 3(b). In order to obtain a high reproducibility with PSNR higher than 30 dB, we found that the uniformly-distributed phase vectors with at least 12^3 lattice points as shown in Fig. 4(a), which can reproduce the image as shown in Fig. 4(b) which was calculated by iterative Fourier transform. One possible method to achieve this is to introduce hole-shaped meta-atoms or meta-atoms using polarized light.

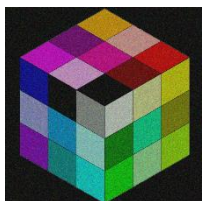


Fig. 2 Target image

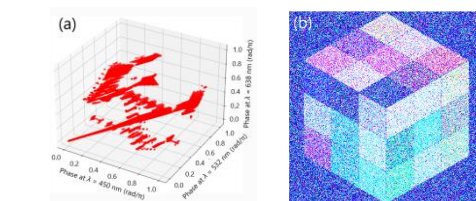


Fig. 3 (a) Phase coverage of our library, and (b) the reproduced image (PSNR = 27.9 dB) (brightness adjusted)

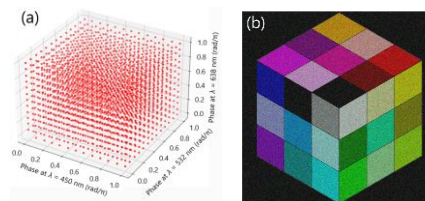


Fig. 4 (a) Uniformly-distributed library, and (b) the simulated image (PSNR = 30.2 dB)

3. Conclusion

In this study, full-color 3D metasurface holograms were designed and simulated. We will proceed with fabrication and evaluation, and aim to improve the reproducibility of the target by incorporating a new shape of meta-atoms to increase the coverage of the phase distribution.

Acknowledgements

We would like to thank Prof. K. Matsushima, the developer of the "WaveField Library" used to calculate the phase distributions.

References

- [1] L. Huang, S. Zhang, T. Zentgraf, "Metasurface holography: from fundamentals to applications", *Nanophotonics*, vol. 7, no. 6, pp. 1169-1190, 2018
- [2] M. Yamaguchi, H. Saito, S. Ikezawa, K. Iwami, "Highly-efficient full-color holographic movie based on silicon nitride metasurface", *Nanophotonics*, vol. 13, no. 8, pp. 1425-1433, 2024
- [3] T. Onozawa, J. Beppu, M. Yamaguchi, K. Iwami, "3D metasurface holograms of SiN for multicolor projection", *The 13th Advanced Lasers and Photon Sources*, 30-03, 2024

A Cost-Effective, Flexible 1D Metasurface Absorber in the Infrared Region

Jhuma Pan¹, Sachin Kumar Srivastava^{1, 2}

¹ Department of Physics, Indian Institute of Technology Roorkee, Uttarakhand, India

² Centre for Photonics and Quantum Communication Technology, Indian Institute of Technology Roorkee, India
E-mail: sachin.srivastava@ph.iitr.ac.in

1. Introduction

Metasurfaces are widely studied to enhance the light absorption in the infrared (IR) spectral regions for their significant importance in space, military and industry applications. Metasurfaces are composed of metal-dielectric structures with subwavelength geometrical parameters and possess the unique capability to manipulate electromagnetic waves in a desired manner. Plasmonic metasurface supports surface plasmon (SP) modes at metal-dielectric interface for the incoming radiation on the structure [1]. The reported IR absorbers utilized complex lithography techniques which increase the overall cost of the absorber. The fabrication of a low-cost, thin and flexible perfect IR absorber using techniques like e-beam lithography (EBL) is still challenging. This study reports an IR absorber based on the excitation of SP mode using an 1D metasurface structure, fabricated by nanoimprint lithography and physical vapor deposition (PVD).

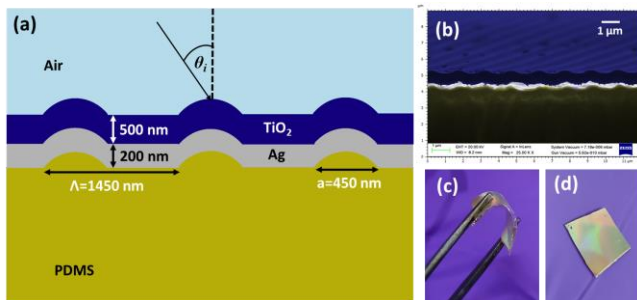


Fig. 1. (a) Schematic of the structure of IR metasurface absorber (b) FE-SEM image of the cross section of the metasurface absorber on a PDMS substrate (Scale bar= 1 μ m). Picture of (c) flexible metasurface absorber being held by a tweezer, (d) uniform and large-area fabricated absorber.

2. Results and Discussions

The metasurface structure consists of an 1D patterned polydimethylsiloxane (PDMS) substrate with a periodic bump of periodicity $\Lambda=1450$ nm. The structure was obtained by templating the polymer over a compact disk (CD). The patterned PDMS substrate was further coated with a thin film of silver (Ag) of about 200 nm thickness, and a titanium dioxide (TiO_2) film of 500 nm thickness using PVD technique. The use of PDMS substrate makes the absorber flexible. Fig.1a shows the schematic of the absorber which is illuminated by an incident light through air at an angle of incidence of θ_i . A field emission scanning electron microscope (FE-SEM) image of the cross-sectional view of the metasurface absorber has been shown in Fig.1b. Ag and TiO_2 layers are clearly visible. The reported thick-

nesses were cited from FE-SEM measurements only. A picture of the fabricated flexible absorber sample is shown in Fig.1c and fig.1d depicts its large area fabrication. The colors in the diffracted light confirm the formation of the nanopatterned structure on the metasurface.

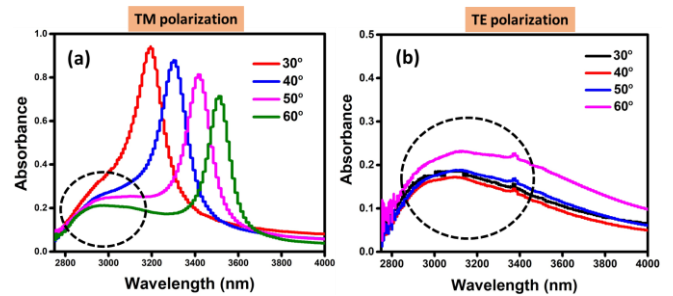


Fig. 2. Experimental absorbance spectra of the metasurface absorber for (a) TM polarized light and (b) TE polarized light at various angle of incidence.

The optical characterization was performed using a Fourier transform infra-red (FTIR) spectrometer equipped with a variable angle specular reflectance accessory and an IR polarizer. Fig.2a shows the measured absorbance spectra for transverse magnetically (TM) polarized light at varying θ_i . Absorbance peak with 94% absorbance is obtained at $\theta_i = 30^\circ$ and a red shift can be observed as the value of θ_i increases from 30° to 60° . Fig.2b shows the absorbance spectra for transverse electrically (TE) polarized light at various θ_i . A circle has been made around a small peak in both Fig.2a and 2b. This small absorbance peak is observed in case of both TM and TE polarized light but the large absorption peak is only present in Fig. 2a for the incidence of TM polarized light. Hence, it can be claimed that the high absorbance is attributed to the excitation of SP mode.

3. Conclusions

A plasmonic metasurface IR absorber with near unity absorbance at large angle of incidence has been demonstrated experimentally. It can be useful in many applications such as refractive index sensor, photodetector, optical filters etc.

Acknowledgements

Funding from MoE-STARs and SERB-SRG grants and IIT Roorkee are thankfully acknowledged.

References

- [1] D. Ray, TV Raziman, C. Santschi, D. Etezadi, H. Altug, O. J. Martin, Nano Letters 20 (2020), 8752-8759.

Polyaniline coated U-bent Fiber Optic Aptasensor for Arsenite Detection in Environmental Matrices

Ashish Shukla^{#1}, Tathagata Pal^{#1}, Soumyo Mukherji^{1*}

¹ Department of Bioscience and Bioengineering, Indian Institute of Technology Bombay

[#] Authors contributed equally

*Corresponding author e-mail: mukherji@iitb.ac.in

Arsenic has been a serious contaminant for decades now. Being the 20th most abundant element on the earth's crust[1], it is found in various organic and inorganic forms. The inorganic form arsenite is known to be the most hazardous to almost all DNA-based life forms[2]. Currently, multiple countries are affected by the elevated concentrations of arsenic contamination [3], [4].

Aptamer as a bio-receptor is a very selective, cost-efficient means for detecting small target analyte [5] such as arsenite oxyanion. Aptamers need certain conditions for their optimum operation. Optical-fiber-based sensors have various advantages such as high sensitivity, small size, lightweight, integration capability, immunity to electrical interference, etc. For absorbance-based fiber-optic sensing, the evanescent wave interaction at the core-cladding interface is a key parameter to achieve high sensitivity in the sensing probe. The cladding can be removed and replaced with the choice of target analyte. The evanescent wave interaction can be improved by bending the optical fiber core in a U shape. To further enhance the sensitivity, the bent fiber core can be coated with conductive polymer e.g., polyaniline. It has been claimed that polyaniline has interesting optical properties. When coated on optical fiber it positively influences evanescent wave-based absorbance in the slightest change of affinity-based interactions. Furthermore, Polyaniline has an immense number of amine groups for crosslinking bioreceptors. These properties lead to the increase of the sensitivity of the fiber-sensing probe significantly.

In the current work, we have developed an aptamer immobilized on a polyaniline-coated U-bent fiber-optic sensor (illustrated in Figure 1) for the detection of arsenite oxyanion in various environmental matrices. The synergistic combination of specificity from aptamer and sensitive combination of polyaniline coating and U-bent fiber gives the sensing probe its ability to detect arsenite in complex water matrices. For this study, the aptamer sequence H₂N-(CH₂)₃-5'-(GT)₂₁-3' was utilized as an arsenic-specific bio-receptor. Under the provided conditions, the arsenic-specific aptamer undergoes formation of tertiary structure that specifically binds to arsenite oxyanion. The optimization of aptamer folding conditions resulted in the sensitive binding of arsenite oxyanion. The aptamer was bound on the polyaniline-coated fiber probe by utilizing a homobifunctional group, glutaraldehyde. The exposed sites on the fiber core were also blocked away by utilizing hexylamine to avoid cross-sensitivity. The optimization of poly-

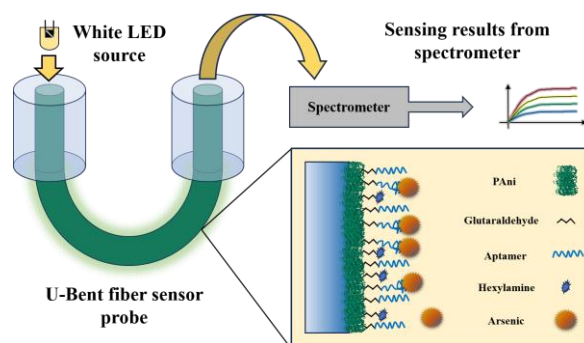


Figure 1: Schematics for the fiber-optic Aptamer based sensing scheme

aniline coating, glutaraldehyde binding and aptamer folding conditions was crucial to achieve the desired sensing results. We were able to get an experimental detection limit of arsenite to as low as 1 ppb in complex environment matrices such as lake water, tap water, etc. The sensing probe gave $R^2 > 0.99$ and a linear range of operation in the range from 1 ppb to 1000 ppb (in log scale). The developed optical fiber aptasensor demonstrates great promise for widescale field deployable arsenic biosensing at low cost.

References

- [1] W. R. Cullen and K. J. Reimer, "Arsenic Speciation in the Environment," *Chemical Reviews*, vol. 89, no. 4, pp. 713–764, 1989, doi: 10.1021/cr00094a002.
- [2] K. P. Raven, A. Jain, and R. H. Loeppert, "Arsenite and arsenate adsorption on ferrihydrite: Kinetics, equilibrium, and adsorption envelopes," *Environmental Science and Technology*, vol. 32, no. 3, pp. 344–349, 1998, doi: 10.1021/es970421p.
- [3] Natasha *et al.*, "Arsenic Environmental Contamination Status in South Asia," *Arsenic in Drinking Water and Food*. Springer Singapore, pp. 13–39, 2020, doi: 10.1007/978-981-13-8587-2_2.
- [4] Y. H. T. Kohda *et al.*, "Arsenic uptake by *Pteris vittata* in a subarctic arsenic-contaminated agricultural field in Japan: An 8-year study," *Science of the Total Environment*, vol. 831, p. 154830, 2022, doi: 10.1016/j.scitotenv.2022.154830.
- [5] M. Kuwahara and N. Sugimoto, "Efficacy of Base-Modi fication on Target Binding of Small Molecule," *Journal of the American Chemical Society*, vol. 135, pp. 9412–9419, 2013.